Photon structure function revisited

Ch. Berger

I. Physikalisches Institut, RWTH Aachen University, 52056 Aachen, Germany[*]

The flux of papers from electron positron colliders containing data on the photon structure function $F_2^\gamma(x, Q^2)$ ended naturally around 2005. It is thus timely to review the theoretical basis and confront the predictions with a summary of the experimental results. The discussion will focus on the increase of the structure function with x (for x away from the boundaries) and its rise with $\ln Q^2$, both characteristics beeing dramatically different from hadronic structure functions. Comparing the data with a specific QCD prediction a new determination of the QCD coupling constant α_s is presented. The agreement of the experimental observations with the theoretical calculations of the real and virtual photon structure is a striking success of QCD.

I. F_2^γ HISTORY, A PERSONAL ACCOUNT

The notion that hadron production in inelastic electron photon scattering can be be described in terms of structure functions like in electron nucleon scattering is on first sight surprising because photons are pointlike particles whereas nucleons have a radius of roughly 1 fm. Nevertheless the concept makes sense, not because the photon consists of pions, quarks, gluons etc, but because it couples to other particles und thus can fluctuate e.g. into a quark antiquark pair or a ρ meson. These two basic processes are distinguished by the terms *pointlike* and *hadronic* throughout the paper. The idea of a photon fluctuating into ρ meson or other vector mesons was soon applied to estimate the inelastic $e\gamma$ scattering cross section in the vector meson dominance model (Brodsky,Kinoshita,Terazawa, 1971; Walsh, 1971). Calculating the structure function in the quark model (Walsh and Zerwas, 1973) then opened the intriguing possibility to investigate experimentally a structure function rising towards large x and showing a distinctive scale breaking because of the proportionality to $\ln Q^2$.

Excitement rose after the first calculation of the leading order QCD corrections, because Witten (1977) not only calculated the markedly different x dependence of the structure function in QCD but demonstrated that the QCD parameter Λ could in principle be determined by measuring an absolute cross section quite in contrast to lepton nucleon scattering, where small scale breaking effects in the Q^2 evolution of the structure function have to be studied. This "remarkable result" (Llewellyn-Smith, 1978) initiated intensive discussions between theorists and experimentalists and passed the first experimental test (PLUTO, 1981) with flying colors. QCD calculations at next to leading order (Bardeen and Buras, 1979; Duke and Owens, 1980) allowed to give Λ a precise meaning in the $\overline{\text{MS}}$ renormalization scheme, but also revealed a sickness of the perturbative calculation, producing negative values of F_2^γ near $x = 0$.

[*]Electronic address: berger@rwth-aachen.de

In an invited talk at the 1983 Aachen conference on photon photon collisions (Duke, 1983) the audience was warned that the implications of these discoveries for the experimental goal of a direct determination of Λ from F_2^γ were not altogether positive despite "the almost incredible advances on the experimental side". Instead it was recommended to utilize the Q^2 evolution like in deep inelastic scattering, a program which was also pursued by other groups (Glück and Reya, 1983).

Ten years later an algebraic error in the original calculation (Bardeen and Buras, 1979) was discovered. Correcting this error (Fontanaz and Pilon, 1992; Glück,Reya,Vogt, 1992) squeezed the negative spike near $x = 0$ to very small x values where it is of negligible practical importance. For the same reason ad hoc attempts (Antoniadis and Grunberg, 1983) to cure the problem (although still in principle important) proved to be unnecessary for experimental analyses.

A new approach to follow the original goal (Albino, Klasen, Söldner-Rembold, 2002) showed promising results. In addition extending the perturbative calculation to NNLO (next to next to leading order) proved the convergence of the perturbative series away from $x = 0$ with small numerical corrections to the NLO result (Moch,Vermaseren,Vogt, 2002). In this review the data are thus compared to NLO predictions only.

II. BASICS

Deep-inelastic electron-photon scattering at high energies

$$e^- + \gamma \rightarrow e^- + \text{hadrons} \,, \tag{1}$$

is characterized by a large momentum transfer Q of the scattered electron and a large invariant mass W of the hadrons. The electron energies E_1 and E_1' in initial and final state combined with the scattering angle θ_1 define the (negative) momentum transfer squared, $-Q^2$, on the electron line with

$$Q^2 = 4E_1 E_1' \sin^2 \theta_1/2 \,. \tag{2}$$

Q^2 and the Bjorken scaling variable x defined as
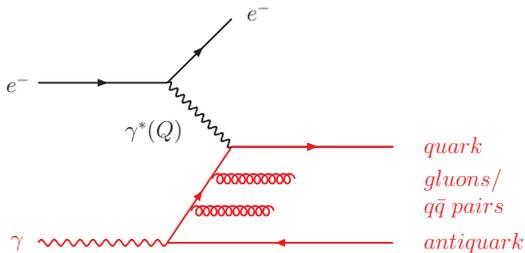
$$x = \frac{Q^2}{Q^2 + W^2} \,, \tag{3}$$

FIG. 1 Electron-photon scattering [generic Feynman diagram]. The incoming target photon γ splits into a nearly collinear quark-antiquark pair. In QCD, the momentum of the internal quark line is reduced by gluon radiation. The impinging electron is scattered off the quark to large angles, the scatter pattern revealing the internal quark structure of the photon. Quark, antiquark and gluons finally fragment to hadrons.

are the essential variables for discussing the dynamics of the scattering process as can be seen from the cross section formula corresponding to Fig. 1

$$\frac{d^2\sigma}{dQ^2dx} = \frac{2\pi\alpha^2}{xQ^4}\left([1+(1-y)^2]F_2^\gamma - y^2 F_L^\gamma\right) \quad (4)$$

which depends on the two structure functions $F_2^\gamma(x,Q^2)$ and $F_L^\gamma(x,Q^2)$. Here F_2^γ is a linear combination $F_2^\gamma = 2x\,F_T^\gamma + F_L^\gamma$ of $F_T^\gamma(x,Q^2)$, describing the exchange of transversely polarized virtual photons, and $F_L^\gamma(x,Q^2)$, associated with the exchange of longitudinally polarized virtual photons. The scaling variable y used in the last equation is given by

$$y = \frac{Q^2}{xs} \quad (5)$$

(with $s = 4EE^\gamma$) and can also be directly calculated from E_1, E_1' and θ_1 via

$$y = 1 - E_1'/E_1 \cos^2\theta_1/2 \ . \quad (6)$$

For QED processes $e\gamma \to e\mu^+\mu^-$ in a region of phase space where one of the muons travels along the direction of the incoming photon and the other is scattered at large angels (balancing the transverse momentum of the outgoing electron) the structure function F_2^γ has been calculated (Budnev et al., 1975; Glück,Reya,Vogt, 1992) to be

$$F_{2,\mathrm{QED}}^\gamma(x,Q^2) = \frac{\alpha}{\pi}x\left(h_1(x,Q^2)\ln\frac{1+\beta}{1-\beta}+h_2(x,Q^2)\right) \quad (7)$$

with $\beta^2 = 1-4M^2x/(1-x)Q^2$ and M denoting the muon mass. The functions $h_1(x,Q^2)$ and $h_2(x,Q^2)$ are given

by

$$h_1 = x^2 + (1-x)^2 + x(1-3x)\frac{4M^2}{Q^2} - x^2\frac{8M^4}{Q^4} \quad (8)$$

$$h_2 = \beta\left(8x(1-x)-1-x(1-x)\frac{4M^2}{Q^2}\right) \ . \quad (9)$$

For heavy quarks with three colors, fractional charge e_q and current masses $M \gg \Lambda$ the right hand side of eq. (7) has to be multiplied by $3e_q^4$. Light quarks have current masses with $M \ll \Lambda$ (or at least $M < \Lambda$). Neglecting all terms $\sim M^2/Q^2$ in eq. (8,9) and respecting $\beta^2 \to 1$ leads for each light quark to the expression

$$F_2^\gamma(x,Q^2) = \frac{3\alpha}{\pi}e_q^4 x\{[x^2+(1-x)^2]\ln\frac{Q^2(1-x)}{xm_0^2}$$
$$+8x(1-x)-1\} \quad (10)$$

where $m_0 \approx 0.3$ GeV is a mass parameter somehow describing the confinement of the light quarks (Walsh and Zerwas, 1973). The QCD parameter Λ can be interpreted as an inverse confinement radius. We therefore replace m_0 by Λ and keep in the leading log approximation only terms proportional to $\ln Q^2$ resulting in

$$F_2^\gamma(x,Q^2) = \frac{3\alpha}{\pi}\sum_{q=u,d,s}e_q^4 x[x^2+(1-x)^2]\ln\frac{Q^2}{\Lambda^2} \quad (11)$$

as the quark model or zero order QCD expression[1] for the photon structure function if only light quarks are considered.
Using the general quark model relation

$$F_2^\gamma(x,Q^2) = 2x\sum_q e_q^2 q^\gamma(x,Q^2) \quad (12)$$

connecting structure function and quark densities q^γ one obtains for light quarks the expression

$$q^\gamma(x,Q^2) = \frac{3\alpha}{2\pi}e_q^2[x^2+(1-x)^2]\ln\frac{Q^2}{\Lambda^2} \quad (13)$$

or

$$q^\gamma(x,Q^2) = \frac{3\alpha}{2\pi}e_q^2 h_{\mathrm{QM}}(x)\ln\frac{Q^2}{\Lambda^2} \quad (14)$$

with

$$h_{\mathrm{QM}}(x) = x^2+(1-x)^2 \ . \quad (15)$$

The factor 2 in eq. (12) accounts for the fact that the photon contains quarks and antiquarks with equal densities but the sum runs over quarks only.

---

[1] A solution which formally requires very high Q^2 (asymptotic solution) and/or staying away from the boundaries $x = 0$ and $x = 1$.

III. QCD PREDICTIONS

A. Introduction, leading order calculations

The first QCD analysis of the photon structure function (Witten, 1977) based on the operator product expansion (OPE) gave a unified picture of the hadronic and pointlike pieces including gluon radiation in leading order. It was shown that the x and Q^2 dependence of F_2^γ is unambiguously calculable for asymptotically high values of Q^2. Due to the $1/\alpha_S$ term in front of the pointlike piece this in turn allows for a determination of the strong coupling constant by measuring an absolute cross section. This unique result was later confirmed by calculations using a diagrammatic ansatz (Llewellyn-Smith, 1978) and/or solving the Altarelli-Parisi equations (DeWitt et al, 1979; Frazer and Gunion, 1979) like in deep inelastic lepton nucleon scattering (DIS). A comprehensive summary of the theoretical foundations has been given by Buras (2006). In this paper we refer to Glück,Reya,Vogt (1992), where the Q^2 evolution equations for massless quarks (and gluons) are solved in the Mellin n-moment space in leading logarithmic order (LO) and next to leading logarithmic order (NLO).

The nth Mellin moment of a function $f(x,Q^2)$ is defined as

$$f^n(Q^2) = \int_0^1 x^{n-1} f(x,Q^2)dx \ . \tag{16}$$

For example, the quark model function $h_{\mathrm{QM}}(x)$ in eq. (15) is projected to

$$h_{\mathrm{QM}}^n = \frac{n^2+n+2}{n(n+1)(n+2)} \ . \tag{17}$$

Like in DIS the quark densities are grouped into two classes described by different evolution equations, flavor non-singlet (NS) and singlet (Σ):

$$
\begin{aligned}
q_{\mathrm{NS}}^\gamma &= \sum_q (e_q^2 - \langle e^2 \rangle)(q^\gamma + \bar{q}^\gamma) \\
\Sigma^\gamma &= \sum_q (q^\gamma + \bar{q}^\gamma) \ ,
\end{aligned}
\tag{18}
$$

where Σ^γ is the first element of a two component singlet parton density q_{S}^γ, composed of Σ^γ and the gluon density G^γ. Here $\langle e^2 \rangle$ is the average charge squared in a system with f quark flavors, e.g. $\langle e^2 \rangle = 2/9$ for $f = 3$. The connection between structure function and quark densities is in LO defined by

$$F_2^\gamma(x,Q^2) = x\left(q_{\mathrm{NS}}^\gamma(x,Q^2) + \langle e^2 \rangle \Sigma^\gamma(x,Q^2)\right) \tag{19}$$

analogous but not identical to the convention defined by eq. (12). Because of the factor x in eq. (19) the mth moment of the structure function is related to the nth moment of the quark densities by

$$F_2^{\gamma,m}(Q^2) = q_{\mathrm{NS}}^{\gamma,n}(Q^2) + \langle e^2 \rangle \Sigma^{\gamma,n}(Q^2) \tag{20}$$

with $m = n - 1$.

We start with a discussion of the LO result for the pointlike $q_{\mathrm{NS}}^{\gamma,n}(Q^2)$, which is given by

$$q_{\mathrm{NS}}^{\gamma,n}(Q^2) = \frac{4\pi}{\alpha_S} a_{\mathrm{NS}}^n(Q^2) \tag{21}$$

with

$$\frac{\alpha_S}{4\pi} = \frac{1}{\beta_0 \ln Q^2/\Lambda^2} \tag{22}$$

and $\beta_0 = 11 - 2f/3$. The finding of Glück,Reya,Vogt (1992) for a_{NS}^n can be written as

$$a_{\mathrm{NS}}^n(Q^2) = \frac{\alpha}{2\pi\beta_0} k_{\mathrm{NS}}^n \frac{1}{1+d_{qq}^n}\left(1 - L^{1+d_{qq}^n}(Q^2)\right) \tag{23}$$

with

$$k_{\mathrm{NS}}^n = 3f(\langle e^4 \rangle - \langle e^2 \rangle^2)2h_{\mathrm{QM}}^n \tag{24}$$

$$d_{qq}^n = \frac{4}{3\beta_0}\left(4\sum_{j=1}^n \frac{1}{j} - 3 - \frac{2}{n(n+1)}\right) \tag{25}$$

and $L(Q^2) = \alpha_S(Q^2)/\alpha_S(Q_0^2)$ giving the ratio of the strong coupling constant at Q^2 and the starting point Q_0^2 of the evolution. In these equations the effect of gluon radiation on the quark model prediction is cast into a simple form. The quark model term k_{NS}^n in eq. (23) is multiplied by a factor accounting for the quark quark splitting in the $q \to qg$ process. The last term in eq. (23) gives a precise meaning to the so called asymptotic solution: a_{NS}^n becomes independent of Q^2 and Q_0^2 in the limit $L \to 0$ i.e. for $Q^2 \to \infty$ or (formally) $Q_0^2 \to \Lambda^2$.

Similar (albeit more complicated) relations hold for $\Sigma^{\gamma,n}(Q^2)$

$$\Sigma^{\gamma,n}(Q^2) = \frac{4\pi}{\alpha_S} a_\Sigma^n(Q^2) \tag{26}$$

with[2]

$$a_\Sigma^n(Q^2) = \frac{\alpha}{2\pi\beta_0} k_q^n \frac{1+d_{gg}^n}{1+d_{PP}^n}\left(1 - L^{1+d_{qq}^n}(Q^2)\right) \tag{27}$$

and

$$k_q^n = 3f\langle e^2 \rangle 2h_{\mathrm{QM}}^n \tag{28}$$

$$d_{PP}^n = d_{qq}^n + d_{gg}^n + d_{qq}^n d_{gg}^n - d_{qg}^n d_{gq}^n \ . \tag{29}$$

The dependence of a_{NS}^n and $\Sigma^{\gamma,n}$ on the parameter Q_0^2 is not expressed explicitly on the left hand side of eq. (23) and eq. (27). The most important consequence of this

---

[2] The derivation of this relatively simple looking form needs some algebraic manipulation of the formula given in Glück,Reya,Vogt (1992).

dependence is the vanishing of the parton densities at the starting scale because $L = 1$ at $Q^2 = Q_0^2$.

Using eq. (25) above as a check of the normalization used in this paper all further splitting terms in equations (23) and (27) can be derived from Glück,Reya,Vogt (1992) and Floratos,Kounnas,Lacaze (1981) quoted therein. Setting $L = 0$ and all $d_{rr'}^n = 0$ with $r, r' \in q, g$ the quark model result

$$F_{2,\text{QM}}^{\gamma,m}(Q^2) = \frac{3\alpha}{\pi} f \langle e_q^4 \rangle h_{\text{QM}}^n \ln \frac{Q^2}{\Lambda^2} \qquad (30)$$

is retained.

The splitting functions $d_{rr'}^n = 0$ (or anomalous dimensions as they are often called following the OPE method) are not restrictetd to integer n values. For example, the harmonic sum $\sum_1^n (1/j)$ in eq. (25) can be interpolated with the help of the Digamma function $\Psi(n)$. There are more complicated harmonic sums contained in the other $d_{rr'}^n$ functions and it is even necessary to continue all n dependent functions in equations (23) and (27) into the complex plane in order to invoke the standard method of inverting the Mellin moments by evaluating the integral

$$F_2^{\gamma}(x, Q^2) = \int_{c-\imath\infty}^{c+\imath\infty} F_2^{\gamma}(m, Q^2) x^{1-m} dm \qquad (31)$$

where m is now a continuous complex variable and the contour c has to lie on the right hand side of the rightmost singularity in $F_2^{\gamma}(m, Q^2)$.
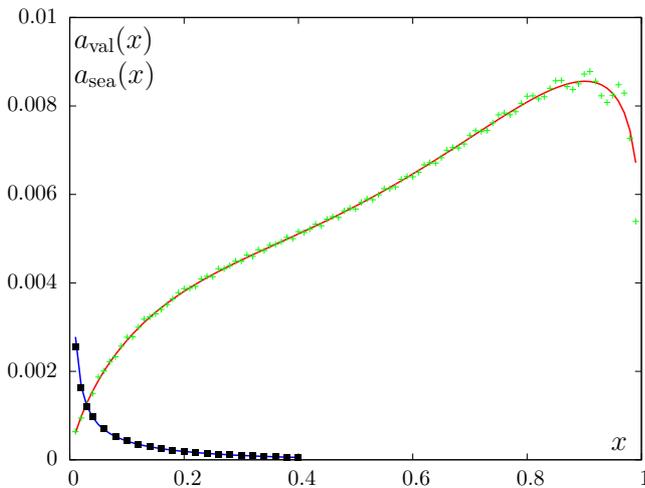

FIG. 2 Upper curve: $a_{\text{val}}(x)$ for $f = 3$. Lower curve: $a_{\text{sea}}(x)$ for $f = 3$. Both curves are calculated with the fitting method described in the text. In addition the crosses and boxes represent the numerical evaluation of the integral (31) in the complex plane.

In practice, instead of inverting $a_{\text{NS}}^n(Q^2)$ and $a_{\Sigma}^n(Q^2)$ the linear combinations

$$a_{\text{val}}^m(Q^2) = \frac{1}{\alpha} \left[\frac{\langle e^4 \rangle}{\langle e^4 \rangle - \langle e^2 \rangle^2} a_{\text{NS}}^n(Q^2) \right] \qquad (32)$$

$$a_{\text{sea}}^m(Q^2) = \frac{1}{\alpha} \left[\langle e^2 \rangle a_{\Sigma}^n(Q^2) - \frac{\langle e^2 \rangle^2}{\langle e^4 \rangle - \langle e^2 \rangle^2} a_{\text{NS}}^n(Q^2) \right]$$

	a_{val}	a_{sea}	b_{val}	b_{sea}
δ	0.7147	-0.70394	0.1046	-1.45262
β	0.1723	0	0.1036	0
c_0	0.0167	0.00011	-0.1199	-0.00024
c_1	-0.0277	-0.00031	-0.1759	-0.00138
c_2	0.0361	0.00028	1.2996	-0.00300
c_3	-0.0010	0.00009	-1.6261	0.01201
c_4	0	0	0.2478	-0.00740

TABLE I Coefficients needed to calculate the pointlike asymptotic contribution to F_2^{γ} according to equations (33) and (36) for 3 flavors ($f = 3$). Each function ($a_{\text{val}}(x)$ etc.) is given by the sum $x^{\alpha}(1-x)^{\beta} \sum_{i=0}^{4} c_i x^i$. Only the first 2 columns are needed for the LO result.

	a_{val}	a_{sea}	b_{val}	b_{sea}
δ	0.6953	-0.71529	0.0858	-1.72537
β	0.1761	0	0.1080	0
c_0	0.0328	0.00033	-0.1535	-0.00061
c_1	-0.0534	-0.00093	-0.4943	0.00153
c_2	0.0695	0.00085	2.6800	-0.02831
c_3	-0.0193	-0.00026	-3.2036	0.05486
c_4	0	0	0.5097	-0.02808

TABLE II Coefficients needed to calculate the pointlike asymptotic contribution to F_2^{γ} according to equations (33) and (36) for 4 flavors ($f = 4$). Each function ($a_{\text{val}}(x)$ etc.) is given by the sum $x^{\alpha}(1-x)^{\beta} \sum_{i=0}^{4} c_i x^i$. Only the first 2 columns are needed for the LO result.

were chosen because the shape of the corresponding *valence* and *sea* distributions in x-space is quite different. Regarding $m = n-1$ the pointlike LO solution in x-space is thus finally given by

$$\frac{1}{\alpha} F_{2,\text{PL}}^{\gamma}(x, Q^2) = \frac{4\pi}{\alpha_S(Q^2)} [a_{\text{val}}(x, Q^2) + a_{\text{sea}}(x, Q^2)] .$$
$$(33)$$

We focus on the asymptotic solution, where a_{val} and a_{sea} do not depend on Q^2. It was found advantageously to follow the inversion method outlined in Duke and Owens (1980), because it quickly leads to analytical expressions for $F_2^{\gamma}(x, Q^2)$ which can be further used in fitting the data. Using the ansatz $x^{\delta}(1-x)^{\beta} \sum_{i=0}^{4} c_i x^i$ for $a_{\text{val}}(x)$ and $a_{\text{sea}}(x)$ the coefficients δ, β, c_i were determined by fitting the moments of these model functions to a_{val}^m and a_{sea}^m respectively. The method can easiliy be extended to nonasymptotic solutions by repeating this procedure for any given pair of Q^2 and Q_0^2.

The results of both inversion methods agree very well, which is demonstrated in Fig. 2, where $a_{\text{val}}(x)$ and $a_{\text{sea}}(x)$ for $f = 3$ have been plotted. The lines were obtained using functions modeling the moments, whereas the points were calculated by numerically evaluating the integral (31) in the complex plane (Zerwas , 2014).

The coefficients necessary for calculating $a_{\text{val}}(x)$ and $a_{\text{sea}}(x)$ are listed in table I for $f = 3$ and table II

for $f = 4$. Note that conventional factors connecting structure functions and quark densities like in equations (12,19) have been absorbed in $a_{\mathrm{val}}(x)$ and $a_{\mathrm{sea}}(x)$.
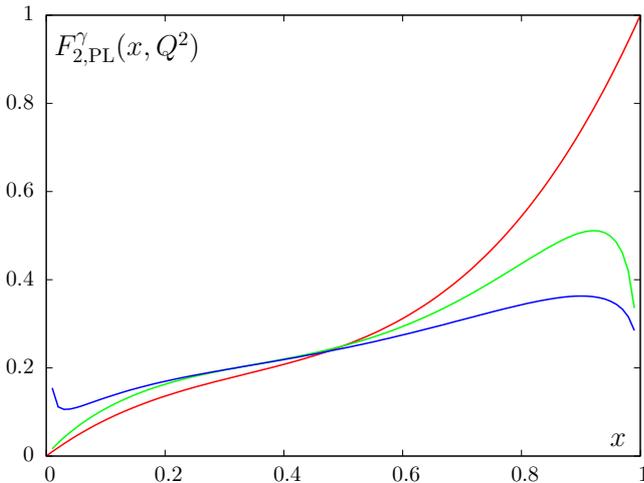

FIG. 3 Red line: quark model (11) in units of N_q according to eq. (34). Blue line: LO QCD prediction (33) in units of N_q/α. Green line: quark model (in units of N_q) as defined in eq. (10) including non leading terms in the logarithm. See text for more details.

Obviously the LO QCD calculation (33) preserves the $\ln Q^2$ behavior of the quark model but changes the x dependence significantly. This is demonstrated in Fig. 3 where $x h_{\mathrm{QM}}(x)$ i.e. the quark model result (11) in units of

$$N_q = \frac{3\alpha}{\pi} \sum_{q=u,d,s} e_q^4 \ln \frac{Q^2}{\Lambda^2} \qquad (34)$$

is compared to the evaluation of eq. (33) in units of N_q/α. The fact that the $\ln Q^2$ behavior of the quark model is preserved, is a consequence of the delicate balance between the increase of the quark population within the photon by the source term $\gamma \rightarrow \bar{q}q$ and the depletion by gluon radiation $q \rightarrow qg$ which however is damped by the decreasing coupling due to asymptotic freedom. Would the coupling be fixed at a non-zero value (Peterson,Walsh,Zerwas, 1983), then the gluon radiation would be so strong that asymptotically the parton densities would fall off to zero as a power for any finite value $x > 0$. Thus, the $\ln Q^2$ rise of the photon structure function is an exciting consequence of asymptotic freedom in QCD. For the same reason, the quark population is depleted at large x by gluon radiation, and the quarks accumulate at small x. As a result, the photon structure function is strongly tilted – a remarkable prediction of perturbative QCD.

To complete the picture, Fig. 3 also contains a QED like variant of the quarkmodel (10) with a log factor $\ln W^2/m_0^2$ instead of $\ln Q^2/\Lambda^2$. With $W^2 = Q^2(1-x)/x$ the curve was calculated for $Q^2 = 100$ GeV^2 and $m_0 = 0.3$ GeV and then divided by N_q using $\Lambda = 0.3$. The

curve is closer to the QCD prediction depending on the new parameter m_0.

Finally a careful inspection of the LO QCD result in Fig. 3 reveals a small upward kink beginning at $x \approx 0.02$, because a_{sea} increases $\sim x^{-0.7}$ for $x \rightarrow 0$. This divergence can be traced back to a pole of a_{Σ}^n (27) when d_{PP}^n approaches -1 for $n < 2$. These poles which plague the perturbative calculations need not concern us as long as they are confined to very small values of x. A closer inspection shows (Berger and Wagner, 1987; Duke, 1983) that they are intimately connected with the rather arbitrary separation of the photon structure function into pointlike and hadron like pieces (see below).

B. Next to leading order calculations

In next to leading order the moments of the parton densities are changed, for example eq. (21) reads now

$$q_{\mathrm{NS}}^{\gamma,n}(Q^2) = \frac{4\pi}{\alpha_S} a_{\mathrm{NS}}^n(Q^2) + \tilde{b}_{\mathrm{NS}}^n(Q^2) \ . \qquad (35)$$

All NLO effects are contained in $\tilde{b}_{\mathrm{NS}}^n(Q^2)$ thus $a_{\mathrm{NS}}^n(Q^2)$ is the leading order result defined in eq. (23). A similar relation holds for $\Sigma^{\gamma,n}(Q^2)$ replacing eq. (26). Besides adding new terms to the parton densities, in NLO the quark model like relation eq. (20) between structure function and quark densities is also changed. Depending on the factorization scheme used the so called Wilson terms have to be added to the right hand side. The lengthy expressions needed to calculate the moments of the structure function in the $\overline{\mathrm{MS}}$ scheme are again all contained in Floratos,Kounnas,Lacaze (1981); Glück,Reya,Vogt (1992). Like for the LO example we prefer to regroup all terms according to the *valence* and *sea* scheme. After inverting the moments the final equation describing the pointlike asymptotic solution

$$\begin{aligned} \frac{1}{\alpha} F_{2,\mathrm{PL}}^{\gamma}(x, Q^2) &= \frac{4\pi}{\alpha_S(Q^2)} [a_{\mathrm{val}}(x) + a_{\mathrm{sea}}(x)] \\ &\quad + b_{\mathrm{val}}(x) + b_{\mathrm{sea}}(x) \end{aligned} \qquad (36)$$

is obtained, where the functions $a_{\mathrm{val}}(x)$, $a_{\mathrm{sea}}(x)$, $b_{\mathrm{val}}(x)$, $b_{\mathrm{sea}}(x)$ can be calculated in a good approximation with the help of tables I,II for $f = 3, 4$. The strong coupling constant now has to be evaluated in NLO

$$\frac{\alpha_S}{4\pi} = \frac{1}{\beta_0 \ln Q^2/\Lambda^2} - \frac{\beta_1}{\beta_0^3} \frac{\ln \ln Q^2/\Lambda^2}{(\ln Q^2/\Lambda^2)^2} \qquad (37)$$

with $\beta_1 = 102 - 38f/3$. Because $F_{2,\mathrm{PL}}^{\gamma}$ and α_S are defined including non leading terms, eq. (36) constitutes an unambiguous QCD prediction in the asymptotic regime depending on one parameter (Λ) only.

The structure of eq. (36) does not change if non asymptotic solutions are considered. One has, however, for each pair of Q^2, Q_0^2-values first to go through the procedure of calculating and inverting the moments including now explicitly Q^2 dependent factors like in eq. (23).
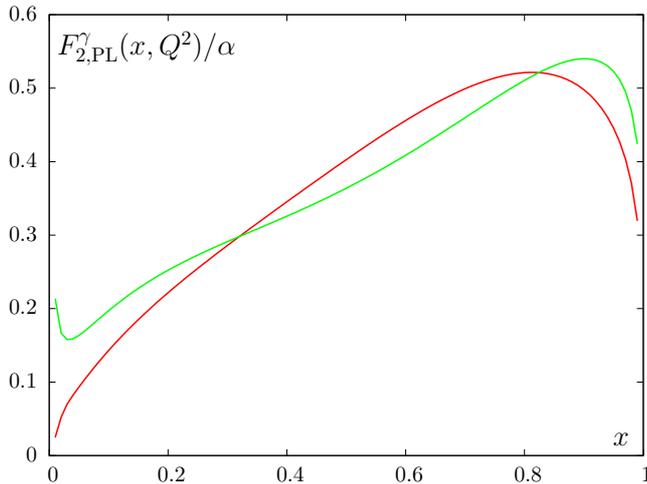
FIG. 4 Comparison of the pointlike structure function $F_{2,\mathrm{pl}}^{\gamma}$ in units of α at leading (green curve) and next to leading order (red curve) QCD for $Q^2 = 100$ GeV^2 and $\Lambda = 300$ MeV.

Due to the negative correction $b_{\mathrm{val}}(x) + b_{\mathrm{sea}}(x)$ at $x \to 1$ the region of high x values is further depleted in NLO as can be seen in Fig. 4 where the LO and NLO results are compared for $f = 3$ and $Q^2 = 100$ GeV^2 with $\Lambda = 300$ MeV. At low x values the NLO correction is also negative and would for $x < 0.01$ even lead to a negative unphysical structure function. This is, however, not problematic because in this regime the measured photon structure function is completely dominated by the hadronic part, which will be discussed in the next section. As mentioned above the negative spikes in F_2^{γ} near $x = 0$ can be attributed to a somewhat artificial separation of pointlike and hadronic pieces.

A further example is studied in Fig. 5 choosing $f = 4$ at $Q^2 = 3$ GeV^2 and $\Lambda = 500$ MeV. $F_{2,\mathrm{PL}}^{\gamma}$ is positive in the whole domain considered (red curve) with a positive sea term $(4\pi/\alpha_S)a_{\mathrm{sea}}(x) + b_{\mathrm{sea}}(x)$ given by the green curve. Due to an algebraic error (Bardeen and Buras, 1979) the moments $b_{\mathrm{sea}}^n(Q^2)$ used in all papers up to 1992 were not correct and resulted in a strongly negative sea term (black curve in Fig. 5) which in turn led to a negative pointlike structure function already for $x < 0.2$ (Duke and Owens, 1980) i.e. much earlier than in the example of Fig. 4. It is not surprising that this finding caused a lot of concern in the literature.

C. Hadroncic piece of F_2^{γ}

The coupling of the photon to the final-state hadrons is mediated by quarks and antiquarks. If the transverse momentum $k_\perp$ in the splitting process $\gamma \to q\bar{q}$ is small, quark and antiquark travel for a large distance $\tau = \sqrt{s}/k_\perp^2$ almost parallel with the same velocity so that strong interactions can develop and bound states form eventually. Associating a light vector meson with this hadronic quantum fluctuation, the corresponding com-
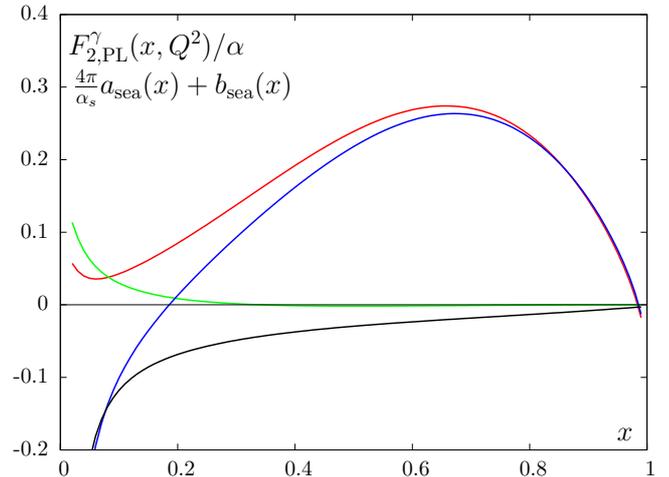

FIG. 5 Red curve: $F_{2,\mathrm{PL}}^{\gamma}$ in units of α for $f = 4$ at $Q^2 = 3$ GeV^2 and $\Lambda = 500$ MeV. Green curve: Sea term $(4\pi/\alpha_S)a_{\mathrm{sea}}(x) + b_{\mathrm{sea}}(x)$ calculated for the same parameters. These curves differ qualitatively from the blue and black curve based on incorrect moments $b_{\mathrm{sea}}^n(Q^2)$.
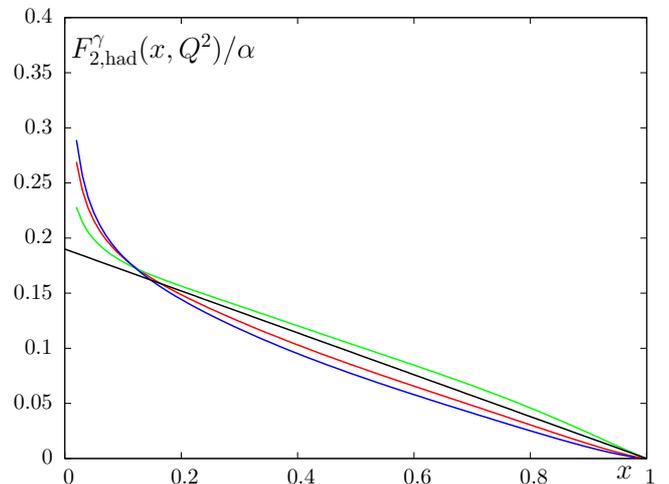

FIG. 6 Shown is the x dependence of $F_{2,\mathrm{had}}^{\gamma}/\alpha$ according to Glück,Reya,Schienbein (1999a) for $Q^2 = 10, 100, 400$ GeV^2 (green, red and blue curves) in comparison with the traditional straight line (black) ansatz $0.19\,(1-x)$.

ponent of the photon wave-function is described by

$$|\gamma\rangle = \frac{\sqrt{\alpha\pi}}{\gamma_\rho}\sqrt{2}\left(\frac{2}{3}|u\bar{u}\rangle - \frac{1}{3}|d\bar{d}\rangle - \frac{1}{3}|s\bar{s}\rangle\right), \qquad (38)$$

which is identical to the vector meson dominance (VMD) ansatz describing the hadronic nature of the photon

$$|\gamma\rangle = \frac{\sqrt{\alpha\pi}}{\gamma_\rho}|\rho\rangle + \frac{\sqrt{\alpha\pi}}{\gamma_\omega}|\omega\rangle + \frac{\sqrt{\alpha\pi}}{\gamma_\phi}|\phi\rangle \qquad (39)$$

if the photon vector meson couplings γ_V are taken from the quark model neglecting mass effects. Preferring the measured couplings $\gamma_\rho, \gamma_\omega, \gamma_\phi$ as determined

from the partial decay width $\Gamma^V_{e^+e^-}$ and utilizing isospin invariance (Glück,Reya,Schienbein, 1999a) $F^\gamma_{2,\mathrm{had}}$ has been tied to the well known pionic quark densities which are available in an easy to use parameterization (Glück,Reya,Schienbein, 1999b).

The result for $F^\gamma_{2,\mathrm{had}}/\alpha$ is shown in Fig. 6 for $Q^2 = 10, 100, 400$ GeV^2. Above $x = 0.1$ there is little variation with Q^2 whereas below $x = 0.1$ the sharp increase indicates the tendency to cancel negative spikes in $F^\gamma_{2,\mathrm{PL}}$. It is interesting to see, how close a simple straight line $F^\gamma_{2,\mathrm{had}}/\alpha = 0.19(1-x)$ approaches the results of the complicated evolution model at $x \geq 0.1$. Straight line models of this sort have been used in the early experimental papers (PLUTO, 1984a).

IV. TWO PHOTON KINEMATICS

Experiments measuring the photon structure function have until now only been performed at e^+e^- storage rings. The reaction

$$e^+ + e^- \rightarrow e^+ + e^- + \mathrm{hadrons} \tag{40}$$

is dominated by the so called *two photon diagram* shown in Fig. 7 which also includes some kinematical definitions. Originally these reactions have been considered only as a background to e^+e^- annihilation ($e^+e^- \rightarrow$ hadrons) but became, due to the absence of high energetic real photon beams, the only source of direct experimental information about $F^\gamma_2(x, Q^2)$.

The incoming leptons in Fig. 7 radiate virtual photons with four momenta q_1, q_2 producing a hadronic system X with an invariant mass $W = \sqrt{(q_1 + q_2)^2}$ The sixfold differential cross section $d^6\sigma/d\boldsymbol{p}'_1 d\boldsymbol{p}'_2$ is given by a complicated combination of kinematical factors and six in principle unknown hadronic functions (four cross sections and two interference terms) depending on W^2, Q^2, P^2. The general formalism has been discussed in great detail in Budnev et al. (1975), which served as the basis of all experimental analyses.

In the limit $P^2 \rightarrow 0$ which is realized by very small forward scattering angles of one of the incoming leptons (e.g. the positron) the relevant formulae are greatly simplified and the cross section reads

$$\frac{d^2\sigma}{d\Omega_1 dE'_1} = \Gamma_t(\sigma_{TT} + \varepsilon\sigma_{LT})f_{\gamma/e}dz \tag{41}$$

with

$$\Gamma_t = \frac{\alpha}{2\pi^2}\frac{E'_1}{Q^2}\frac{1+(1-y)^2}{y} \tag{42}$$

$$\varepsilon(y) = \frac{2(1-y)}{1+(1-y)^2} \tag{43}$$

and

$$f_{\gamma/e}(z, \theta_{2,\mathrm{max}}) = \frac{\alpha}{\pi z}\big([1+(1-z)^2] \tag{44}$$

$$\cdot \ln\left(\frac{E(1-z)}{mz}\theta_{2,\mathrm{max}}\right) - 1 - z\big)$$

where the definition $z = (E_2 - E'_2)/E_2$ has been used.

The two photon cross sections σ_{TT} and σ_{LT} depend on Q^2 and W^2. The indices represent the transverse (T) and longitudinal (L) polarization of the virtual photons.
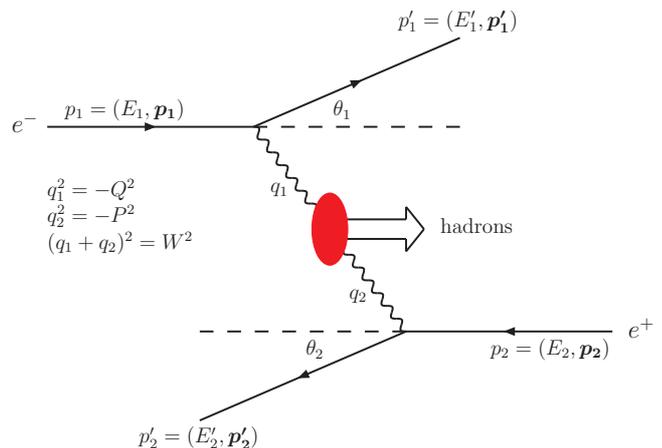

FIG. 7 Kinematics of the two photon process

The physical interpretation of these equations is like follows: the incoming positron is replaced by a beam of quasi real photons with transverse polarization traveling along the positron direction. The number of photons in the energy interval dz is given by $f_{\gamma/e}dz$. The term $\Gamma_t d\Omega_1 dE'_1$ denotes the number of transversely polarized photons radiated from the electron scattered into the solid angle and energy interval $d\Omega_1 dE'_1$ at angles $\theta_1 \gg \theta_2$. With the help of the polarization parameter ε the number of longitudinal photons is given by $\varepsilon\Gamma_t$. A very useful feature of this formalism is the factorization of the flux factors into $\Gamma_t \cdot f_{\gamma/e}$ and $\varepsilon\Gamma_t \cdot f_{\gamma/e}$ where Γ_t and ε depend on electron variables and $f_{\gamma/e}$ on positron variables only. This allows for a considerable simplification calculating the photon fluxes in Monte Carlo routines simulating the experiments. It has been shown (Berger and Field, 1981) that for $\theta_2 < 20$ mrad the numerical difference in evaluating the incoming photon densities from this approach or from the exact formula (Budnev et al., 1975) is less than 0.5% for $W/2E > 0.05$.

Replacing the cross sections σ_{TT}, σ_{LT} by the structure functions

$$F^\gamma_2(x, Q^2) = \frac{Q^2}{4\pi\alpha^2}(\sigma_{TT} + \sigma_{LT}) \tag{45}$$

$$F^\gamma_L(x, Q^2) = \frac{Q^2}{4\pi\alpha^2}\sigma_{LT}$$

we arrive after a change of variables at

$$\frac{d^3\sigma}{dQ^2 dx dz} = \frac{2\pi\alpha^2}{xQ^4}\big([1+(1-y)^2]F_2^\gamma - y^2 F_L^\gamma\big)f_{\gamma/e} \quad (46)$$

which corresponds to eq. (4) multiplied by the spectral density of the incoming photons. Under actual experimental conditions, y is quite small in general, so that F_L^γ is very difficult to measure. Experiments usually focus on the measurement of F_2^γ and neglect F_L^γ. This is theoretically backed further by the fact that quark model and QCD predict F_2^γ to be the leading component.

The standard expression (44) has first been derived by Kessler (1960). In the spirit of the leading log approximation it can be replaced by

$$f_{\gamma/e}(z, \theta_{2,\max}) = \frac{\alpha}{\pi z}[1+(1-z)^2]\ln\frac{E}{m} \qquad (47)$$

useful for rough estimates of the counting rate. One has, however, to keep in mind that neglecting the cutoff $\theta_{2,\max}$ has not only numerical consequences, but quickly violates the basic assumption $P^2 \approx 0$. It is difficult to quote unambiguous limits for the maximum allowed mean P^2 values. Detailed calculation of μ pair production (Nisius, 2000) revealed that for $E = 45$ GeV and $\theta_{2,\max} = 27$ mrad one has $\langle P^2\rangle = 0.04$ GeV^2 and 97% of the cross section is contained in eq. (41), a result which is likely also to be valid for the quark model and QCD. It follows that the experiments need forward spectrometers with electromagnetic calorimeters very close to the beam pipe which allow to reject positrons with angles larger than about 25 mrad via the method of antitagging.

The basic experimental procedure is thus given by investigating the reaction $e^+e^- \to e^+e^- +$ hadrons with the electron scattered at angles larger than $\theta_{2,\max}$ and the positron traveling undetected down the beam pipe (and vice versa). Due to the unknown energy E_2' of the outgoing positron E_γ is also not known and the usual relation $Q^2 = xys$ cannot be used for calculating x. Therefore hadronic calorimeters reaching down to small forward scattering angles are needed in order to measure the invariant mass W of the produced hadronic system and calculate x from eq. (3). Unfortunately the remnants of the antiquark in Fig. 1 will also be dominantly concentrated at small angles and losses in the hadronic energy are unavoidable. With $W_{\exp} \leq W_{\text{true}}$ sophisticated unfolding methods have to be employed in order to reconstruct x. These methods are described in the experimental publications and reviewed in Berger and Wagner (1987); Nisius (2000). A discussion of the various Monte Carlo routines used by the different experimental groups in evaluating the cross section can e.g. be found in Nisius (2000).

V. EXPERIMENTAL ANALYSIS

Following the pioneering work of the PLUTO collaboration (PLUTO, 1981) many experiments have been performed at all high energy e^+e^- storage rings. In order to avoid the region of small x with its mixture of correlated hadronic and pointlike contributions we exclude data with $x \leq 0.1$. Data where the charm component has been subtracted and all data published in conference proceedings only are also discarded. This selection leads to 109 experimental values of $F_2^\gamma(x, Q^2)/\alpha$ with Q^2 values ranging from 4.3 GeV^2 to 780 GeV^2 from the collaborations ALEPH (ALEPH, 1999, 2003), AMY (AMY, 1995, 1997), DELPHI (DELPHI, 1996), JADE (JADE, 1984), L3 (L3, 1998, 1999, 2000, 2005), OPAL (OPAL, 1997a,b, 2002), PLUTO (PLUTO, 1984a, 1987), TASSO (TASSO, 1986), TOPAZ (TOPAZ, 1994) and TPC/2γ (TPC/2γ, 1987). In cases where the experimental uncertainties could only be read off the figures the tables of Nisius (2000) were used. As usual the experimental x and Q^2 values are obtained from an averaging procedure over the sometimes rather large x and Q^2 bins. In most cases x coincides with the bin center.

After the 1980 crisis of the perturbative calculation most QCD analyses were performed like in deep inelastic scattering by comparing the data to models obtained by evolving the parton densities from a starting scale $Q_0^2 \gg \Lambda^2$ up to Q^2. For a recent extensive study see Cornet, Jankowski, Krawczyk (2004). On the other hands side data at high Q^2 and high x (defined by $Q^2 \geq 59$ GeV^2 and $x \geq 0.45$) were fitted to the asymptotic pointlike solution (36) for $f = 3$, supplemented by the quark model formula (7) for a charm quark with mass 1.5 GeV (Albino, Klasen, Söldner-Rembold, 2002). The fit described the data very well and resulted in $\alpha_S(M_Z) = 0.1183 \pm 0.0058$ with $\chi^2 = 9.1$ for 20 experimental data.

Here we follow a more radical approach and fit the whole sample of 109 data sets to a model whose three components have been discussed in the previous sections:

1. The pointlike (PL) asymptotic NLO QCD prediction (36) for 3 light flavors in the $\overline{\text{MS}}$ scheme with Λ_3 as the only free parameter using the coefficients of table I. We emphasize again that this result is contained in the general solution (Glück,Reya,Vogt, 1992) for $L = 0$ (i.e. Q_0^2 very close to Λ^2 as choice for the starting scale).

2. A quark model calculation of the charm and bottom quark contribution using eq. (7) multiplied by $3e_q^4$. Applying the $\overline{\text{MS}}$ scheme for the QCD calculation it is only natural to use the $\overline{\text{MS}}$ masses $M_c = 1.275 \pm 0.025$ GeV and $M_b = 4.18 \pm 0.03$ GeV as quoted by the Particle Data Group (PDG, 2012).

3. A detailed parameterization for the hadronic part of the structure function (Glück,Reya,Schienbein, 1999b) including the Q^2 evolution. Examples for different values of Q^2 are displayed in Fig. 6.

The high quality fit ($\chi^2_{\text{dof}} = 78/108$) results in a value of $\Lambda_3 = 0.338 \pm 0.020$ GeV. Following the method explained in Marciano (1984) this value is converted to
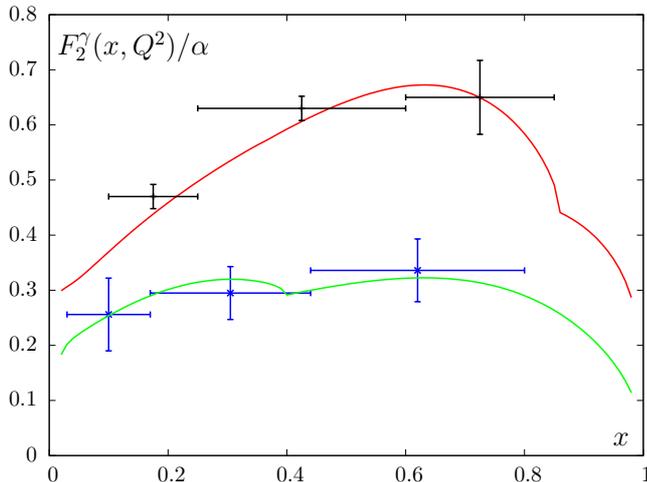
FIG. 8 Dependence of F_2^γ/α on x for two different values of Q^2. The PLUTO data (PLUTO, 1984a) at 4.3 GeV^2 (blue crosses) and the OPAL data (OPAL, 2002) at 39.7 GeV^2 (black crosses) are compared with the QCD model described in the text (green and red curves).

FIG. 9 Dependence of F_2^γ/α on Q^2. All available data for F_2^γ/α with $0.3 < \bar{x} < 0.5$ are averaged in Q^2 bins with equal width in $\ln Q^2$ as explained in the text. The red curve shows the result of our QCD model.

$\Lambda_5 = 0.201 \pm 0.015$ GeV and therefore $\alpha_S(M_Z^2) = 0.1159 \pm 0.0013$ is obtained in NLO where the error only reflects the experimental uncertainties. In order to estimate the theoretical error we first neglected the bottom quark contribution which changes $\alpha_S(M_Z^2)$ by a very small amount (0.0002). Varying M_c within the quoted error of ± 0.0025 GeV resulted in $\Delta\Lambda_3 = \pm 0.007$. The most important source of theoretical uncertainty is the treatment of the hadronic contribution. This error is hard to estimate. Possible interferences between hadronic and pointlike part are very likely restricted to the region $x \leq 0.1$ which is excluded by our data selection. Glück,Reya,Schienbein (1999b) emphasize the very good agreement of their result with pionic and photonic structure function data. Assuming a 10% normalization error for $F_{2,\mathrm{had}}^\gamma/\alpha$ yields $\Delta\Lambda_3 = \pm 0.042$. Adding all errors in quadrature the final result is

$$\alpha_S(M_Z^2) = 0.1159 \pm 0.0030 \qquad (48)$$

which agrees nicely with the DIS average $\alpha_S(M_Z^2) = 0.1151 \pm 0.0022$ and the world average $\alpha_S(M_Z^2) = 0.1184 \pm 0.0007$ as given in PDG (2012).

In order to visualize the impressive agreement between data and theory two examples are presented. In Fig. 8 the PLUTO data (PLUTO, 1984a) at 4.3 GeV^2 (black crosses) and the OPAL data (OPAL, 2002) at 39.7 GeV^2 (blue crosses) are compared with our model. The data clearly do not follow the typical mesonic $1 - x$ dependence and also demonstrate implicitly the rather strong Q^2 dependence predicted by QCD.

Next the Q^2 dependence of $F_2^\gamma(x, Q^2)$ is directly tested by selecting data with $0.3 < \bar{x} < 0.5$. The average x value $\bar{x}$ was determined taking the mean value of the x intervals quoted in the experimental papers. The 36 data sets are grouped in bins with equal bin width in
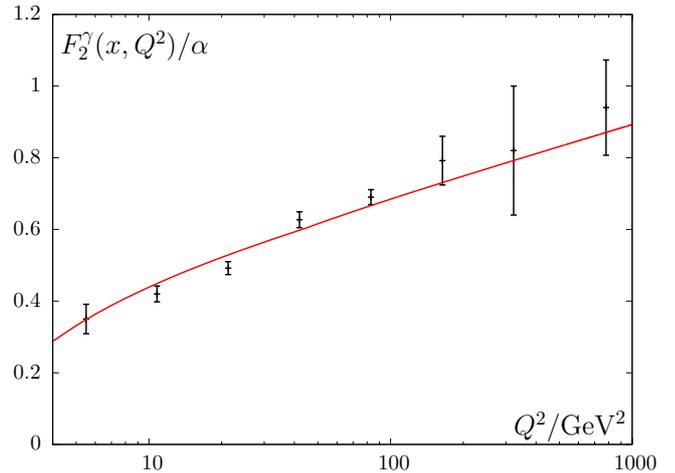
$\ln Q^2$. Each F_2^γ value is then shifted to the center of the corresponding bin using the theoretical model and the weighted average of all data within the bin is calculated. The result is shown in Fig. 9 together with the theoretical curve calculated for $x = 0.4$. The increase of the data with $\ln Q^2$ is clearly seen, especially in contrast to the well known slight *decrease* of the proton structure function for $x = 0.4$ between $Q^2 = 5$ and 800 GeV^2. Neglecting the small Q^2 dependence of the hadronic piece the theoretical model can in LO be written as $F_2^\gamma(x, Q^2) = a(x) + b(x) \ln(Q^2/\mathrm{GeV}^2)$. A fit of the data in Fig. 9 according to this ansatz yields $b(0.4) = 0.133 \pm 0.008$ thus establishing numerically the predicted increase with $\ln Q^2$ beyond any doubt. This value agrees very well with the earlier analysis of Nisius (2000).

VI. VIRTUAL PHOTON STRUCTURE

The perturbative calculations have been extended to the region $\Lambda^2 \ll P^2 \ll Q^2$ (Uematsu,Walsh, 1981, 1982) which is experimentally accessible requesting also the positron being scattered into finite angles (double tagging). Regarding the theory one has in the formalism of Glück,Reya,Vogt (1992) simply to replace the parameter Q_0^2 by the variable P^2 for the calculation of $F_{2,\mathrm{PL}}^{\gamma,n}(Q^2, P^2)$.

Gluon radiation is efficiently suppressed for virtual photons thus moving $F_2^{\gamma(P^2)}(x, Q^2)$ closer to the quark model result. Analytically this can be proven easily (Uematsu,Walsh, 1981) by investigating the LO order solution, e.g. $q_{\mathrm{NS}}^{\gamma,n}$, eq. (21). Because in LO α_S is
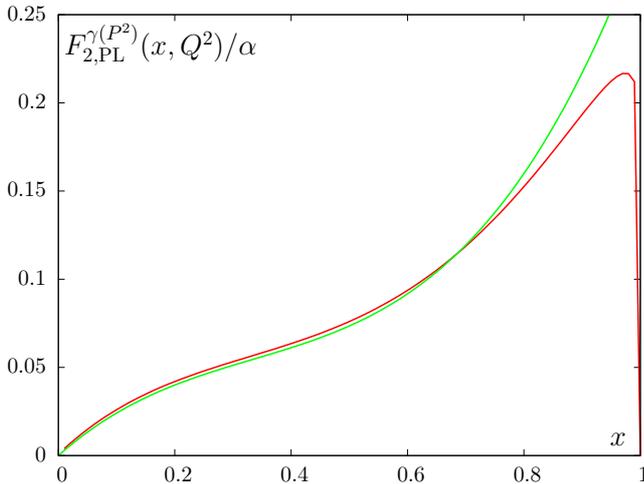
FIG. 10 Dependence on x of the virtual photon structure function $F_2^{\gamma(P^2)}(x,Q^2)/\alpha$ calculated in LO for $Q^2 = 30$ GeV^2, $P^2 = 7.5$ GeV^2 and $\Lambda_3 = 0.338$ GeV (red curve) in comparison (green curve) with the modified quark model result derived from eq. (50).

proportional to $1/\ln(Q^2/\Lambda^2)$ we have

$$q_{\mathrm{NS}}^{\gamma,n} \sim \frac{\ln\frac{Q^2}{\Lambda^2} - \ln\frac{P^2}{\Lambda^2}\left(\frac{\ln(P^2/\Lambda^2)}{\ln(Q^2/\Lambda^2)}\right)^{d_{qq}^n}}{1 + d_{qq}^n} \ . \qquad (49)$$

Using $\ln(Q^2/\Lambda^2) = \ln(P^2/\Lambda^2) + \ln(Q^2/P^2)$ the nominator reduces in the limit $\ln(Q^2/P^2) \ll \ln(P^2/\Lambda^2)$ to $(1 + d_{qq}^n)\ln(Q^2/P^2)$. Since a similar relation holds for the singlet term, the final result[3] is

$$F_{2,\mathrm{PL}}^{\gamma,n}(Q^2,P^2) = \frac{3\alpha}{\pi} f\langle e_q^4\rangle h_{\mathrm{QM}}^n \ln\frac{Q^2}{P^2} \ , \qquad (50)$$

i.e. the quark model formula (30) with the log factor replaced by $\ln(Q^2/P^2)$. As an illustration the LO prediction for $Q^2 = 30$ GeV^2, $P^2 = 7.5$ GeV^2 and $\Lambda_3 = 0.338$ GeV is compared in Fig. 10 with eq. (50) showing perfect agreement at small and medium x values. The parameter free QCD prediction (50) is, however, difficult to be tested experimentally because with the present value of Λ the condition $\ln(Q^2/P^2) \ll \ln(P^2/\Lambda^2)$ can hardly be achieved.

Regarding the determination of $F_2^{\gamma(P^2)}(x,Q^2)$ from the measured cross section, it should be remembered that the virtual photon photon scattering is in general described by four cross sections and two interference terms (see section IV). After proper integration over the interference terms the cross section formula of Budnev et al. (1975)

---

[3] This formula also demonstrates drastically how the introduction of a second scale destroys the sensitivity to Λ. In case of the starting scale Q_0^2 of section III with values of 0.3 to 1.0 GeV^2 a reduced sensitivity is maintained.
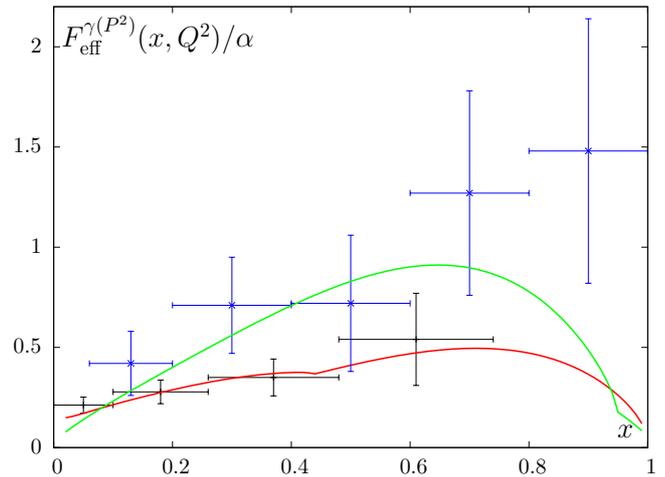

FIG. 11 Shown is the x dependence of $F_{\mathrm{eff}}^{\gamma(P^2)}(x,Q^2)/\alpha$. The PLUTO data at $Q^2 = 5$ GeV^2, $P^2 = 0.35$ GeV^2 (black crosses) are compared to the QCD prediction (red curve) including hadronic and charm quark contributions. The details are explained in the text. The L3 data at $Q^2 = 120$ GeV^2, $P^2 = 3.7$ GeV^2 (blue crosses) are compared to the same model (green curve).

can be written as

$$d\sigma \sim L_{TT}(\sigma_{TT} + \varepsilon_1\sigma_{LT} + \varepsilon_2\sigma_{TL} + \varepsilon_1\varepsilon_2\sigma_{LL}) \qquad (51)$$

where the factor L_{TT} is approximately interpreted as describing the fluxes of transverse virtual photons from the incoming electron and positron. The polarization parameters ε_1 and ε_2 are for typical experimental conditions close to 1 and therefore

$$d\sigma \sim L_{TT}(\sigma_{TT} + \sigma_{LT} + \sigma_{TL} + \sigma_{LL}) \ . \qquad (52)$$

The relation between structure functions and cross sections is more complicated than discussed above for electron scattering off real photons. In the limit $Q^2 \gg P^2$ the general formulae given in Berger and Wagner (1987) reduce to

$$F_2^{\gamma(P^2)}(x,Q^2) = \frac{Q^2}{4\pi\alpha^2}(\sigma_{TT} + \frac{1}{2}\sigma_{LT}) \qquad (53)$$

$$F_L^{\gamma(P^2)}(x,Q^2) = \frac{Q^2}{4\pi\alpha^2}\sigma_{LT}$$

using $\sigma_{LT} \approx \sigma_{TL}$ and $\sigma_{LL} \approx 0$. Defining an effective structure function via

$$F_{\mathrm{eff}}^{\gamma(P^2)} = \frac{Q^2}{4\pi\alpha^2}(\sigma_{TT} + \sigma_{LT} + \sigma_{TL} + \sigma_{LL}) \qquad (54)$$

one gets finally

$$F_{\mathrm{eff}}^{\gamma(P^2)}(x,Q^2) \approx F_2^{\gamma(P^2)}(x,Q^2) + \frac{3}{2}F_L^{\gamma(P^2)}(x,Q^2) \ . \ (55)$$

Experimental data is scarce. The first results of the PLUTO collaboration (PLUTO, 1984b) at $Q^2 = 5$ GeV^2

and $P^2 = 0.35$ GeV^2 (black crosses in Fig. 11) were only followed by data of the L3 collaboration (L3, 2000) at $Q^2 = 120$ GeV^2 and $P^2 = 3.7$ GeV^2 (blue crosses in Fig. 11).

For comparison with theory $F_2^{\gamma(P^2)}(x, Q^2)$ is calculated for 3 flavors choosing $\Lambda_3 = 0.338$ GeV. According to eq. (55) $F_L^{\gamma(P^2)}(x, Q^2)$ cannot be neglected. The longitudinal structure function of real photons is extensively discussed in the literature (Laenen et al. , 1994). A QCD calculation not being at hand, $F_L^{\gamma(P^2)}(x, Q^2)$ is approximated for light quarks by the quark model result quoted in Glück,Reya,Schienbein (1999a). The same authors argue that the charm quark contribution should also be adopted from the real photon case. The VMD contribution for $P^2 \neq 0$ has to be multiplied by a form factor $1/(1 + P^2/m_\varrho^2)^2$ where m_ϱ is the ϱ meson mass. This form factor practically cancels the hadronic contribution to the L3 data. Regarding the PLUTO data the VMD term is reduced by a factor 3 and thus for the sake of simplicity the straight line model $0.19(1 - x)/3$ is applied. The red curve (PLUTO) and the green curve (L3) in Fig. 11 are in very good agreement with the data although admittedly this is not a very decisive test due to the large experimental errors.

Conclusion

Measurements of the photon structure function F_2^γ taken at e^+e^- colliders were confronted with a theoretical model. The main component is the fixed flavor ($f = 3$) NLO asymptotic QCD result in the $\overline{\text{MS}}$ scheme as given in Glück,Reya,Vogt (1992) by choosing Q_0^2 close to Λ^2. This part is complemented by charm and bottom heavy quark contributions calculated in the quark model and by a hadronic contribution taken from vector meson dominance. The model describes not only the x and Q^2 distributions very well but also allows for a precise determination of the strong coupling constant, yielding $\alpha_S(M_Z^2) = 0.1159 \pm 0.0030$. The excellent agreement between data and theory and the absence of negative spikes in $F_{2,\text{PL}}^\gamma(x, Q^2)$ for $x \geq 0.01$ contradicts the argument that that a meaningful determination of $\alpha_S(M_Z^2)$ is only possible via measuring the Q^2 evolution of the photon structure function analogous to lepton nucleon scattering.

New experimental input can only be expected from a new high energy e^+e^- collider. At the planned linear collider ILC (ILC, 2014) it is in principle possible to install a high intensity beam of real photons via backscattering of laser light. This would for the first time allow to study inelastic electron photon scattering in a beam of real photons with a spectrum and intensity far superior to the virtual photons used until now (Muhlleitner, Zerwas, 2006). In addition nagging doubts about the P^2 cutoff in some of the two photon experiments are baseless in such an environment.

References

Albino, S., M. Klasen and S. Söldner-Rembold, 2002, Phys. Rev. Lett. **89**, 122004-1

ALEPH Collaboration, R. Barate et al., 1999, Phys. Lett. **B458**, 152

ALEPH Collaboration, A. Heister et al., 2003, European Physical Journal **C30**, 145

AMY Collaboration, S.K. Sahu et al., 1995, Phys. Lett. **B346**, 208

AMY Collaboration, T. Kojima et al., 1997, Phys. Lett. **B400**, 395

Antoniadis, I. and G. Grunberg, 1983, Nucl. Phys. **B213**, 445

Bardeen, W.A. and A.J. Buras, 1979, Phys. Rev. **D20**, 166, [Erratum ibid. **D21**, 2041, 1980]

Berger, Ch. and J. Field, 1981, Nucl. Phys. **B187**, 585

Berger, Ch. and W. Wagner, 1987, Physics Reports **146**, 1

Brodsky, S.J., T. Kinoshita and H. Terazawa, 1971, Phys. Rev. Lett. **27**, 280

Budnev, V.M. et al., 1975, Physics Reports **15**, 181

Buras, A.J., 2006, Acta Phys. Polon. **B37**, 609, and hep-ph/0512238

Cornet, F., P. Jankowski and M. Krawczyk, 2004, Phys. Rev. **D70**, 093004-1

DELPHI Collaboration, P. Abreu et al., 1996, Z. Phys. **C69**, 223

DeWitt, R.J. et al., 1979, Phys. Rev. **D19**, 2046, [Erratum ibid. **D20**, 1751, 1979]

Duke, D.W. and J.F. Owens, 1980, Phys. Rev. **D22**, 2280

Duke, D.W., 1983, Photon Photon Collisions, Proceeding of the Fifth International Workshop on Photon Photon Collisions, ed. Ch. Berger, Lecture Notes in Physics 191, Springer Verlag, Germany

Fontanaz, M. and E. Pilon, 1992, Phys. Rev. **D45**, 382

Floratos, E.G., C. Kounnas and R. Lacaze, 1981, Nucl. Phys. **B192**, 417

Frazer, W.R. and J.F. Gunion, 1979, Phys. Rev. **D20**, 147

Glück, M. and E. Reya, 1983, Phys. Rev. **D28**, 2749

Glück, M., E. Reya and A. Vogt, 1992, Phys. Rev. **D45**, 3986

Glück, M., E. Reya and I. Schienbein, 1999, Phys. Rev. **D60**, 054019

Glück, M., E. Reya and I. Schienbein, 1999, Eur. Phys. J **C10**, 313

ILC Collaboration, J. Bagger et al., 2014, The International Linear Collider, Gateway to the Quantum Universe Committee, http://www.linearcollider.org/pdf/ilc_gateway_report.pdf

JADE Collaboration, W. Bartel et al., 1984, Z. Phys. **C24**, 231

Kessler, P., 1960, Nuovo Cimento **17**, 809

Laenen, E. et al., 1994, Phys. Rev. **D49**, 5753

L3 Collaboration, M. Acciarri et al., 1998, Phys. Lett. **B436**, 403

L3 Collaboration, M. Acciarri et al., 1999, Phys. Lett. **B447**, 147

L3 Collaboration, M. Acciarri et al., 2000, Phys. Lett. **B483**, 373

L3 Collaboration, M. Acciarri et al., 2005, Phys. Lett. **B622**, 249

Llewellyn-Smith, C.H., 1978, Phys. Lett. **B79**, 83

Marciano, W.J., 1984, Phys. Rev. **D29**, 580, 1983

Moch, S., J.A. Vermaseren and A. Vogt, 2002, Nucl. Phys. **B621**, 413, 2002, [hep-ph/0110331] and A. Vogt, S.Moch and J. Vermaseren, Acta Phys. Polon. **B37**, 683, 2006 [hep-ph/0511112]

Muhlleitner, M.M., and P.M. Zerwas, 2006, Acta Phys. Polon. **B37**, 1021, [hep-ph/0511339]

Nisius, R., 2000, Physics Reports **332**, 165

OPAL Collaboration, K. Ackerstaff et al., 1997, Z. Phys. **C74**, 33

OPAL Collaboration, K. Ackerstaff et al., 1997, Phys. Lett. **B411**, 387

OPAL Collaboration, G. Abbiendi et al., 2002, Phys. Lett. **B533**, 207

Particle Data Group, J. Beringer et al., 2012, Phys. Rev. **D86**, 010001 and online http://pdg.lbl.gov /2012/listings/contents_listings.html

Peterson, C., T.F. Walsh and P.M. Zerwas, 1983, Nucl. Phys. **B229**, 301

PLUTO Collaboration, Ch. Berger et al., 1981, Phys. Lett. **B107**, 168

PLUTO Collaboration, Ch. Berger et al., 1984 Phys. Lett. **B142**, 111

PLUTO Collaboration, Ch. Berger et al., 1984, Phys. Lett. **B142**, 119

PLUTO Collaboration, Ch. Berger et al., 1987, Nucl. Phys. **B281**, 365

TASSO Collaboration, M. Althoff et al., 1986, Z. Phys. **C31**, 527

TOPAZ Collaboration, K. Muramatsu et al., 1994, Phys. Lett. **B332**, 477

TPC/2γ Collaboration, H. Aihara et al., 1987, Z. Phys. **C34**, 1

Uematsu, T. and T.F. Walsh, 1981, Phys. Lett. **B101**, 263

Uematsu, T. and T.F. Walsh, 1982, Nucl. Phys. **B199**, 93

Walsh, T.F., 1971, Phys. Lett. **B36**, 121

Walsh, T.F. and P.M. Zerwas, 1973, Phys. Lett. **B44**, 195

Witten, E., 1977, Nucl. Phys. **B120**, 189

Zerwas, P.M., 2014, private communication